Relation between torsion and cross-sectional area change in the human left ventricle

ELSEVIER

PII: S0021-9290(96)00147-9

J. Biomechanics, Vol. 30, No. 3, pp. 207–212, 1997

Printed in Great Britain
0021-9290/97 $17.00 + .00

RELATION BETWEEN TORSION AND CROSS-SECTIONAL AREA CHANGE IN THE HUMAN LEFT VENTRICLE

F. W. L. Aelen,* T. Arts,* D. G. M. Sanders,† G. R. P. Thelissen,† A. M. M. Muijtjens,‡ F. W. Prinzen§ and R. S. Reneman§

Departments of *Biophysics, §Physiology and ‡Medical Informatics, Cardiovascular Research Institute Maastricht, Maastricht University, Maastricht, The Netherlands; and †Department of Diagnostic Radiology, University Hospital Maastricht, Maastricht, The Netherlands

Abstract—During the ejection phase, motion of the left ventricular (LV) wall is such that all myocardial fibers shorten to the same extent. In a mathematical model of LV mechanics it was found that this condition could be satisfied only if torsion around the long axis followed a unique function of the ratio of cavity volume to wall volume. When fiber shortening becomes non-uniform due to cardiac pathology, this pathology may be reflected in aberration of the torsional motion pattern. In the present study we investigated whether the predicted regular motion pattern could be found in nine healthy volunteers, using Magnetic Resonance Tagging. In two parallel short-axis cross-sections, displacement, rotation, and area ejection were derived from the motion of tags, attached non-invasively to the myocardium. Information from both sections was combined to determine area ejection, quantified as the change in the logarithm of the ratio of cavity area to wall area, and torsion, represented by the shear angle on the epicardium. Linear regression was applied to torsion as a function of area ejection. The slope thus found (-0.173 ± 0.024 rad, mean $\pm$ S.D.) was similar to the slope as predicted by the model of LV mechanics (-0.194 ± 0.026 rad). In conclusion, the relation between area ejection and torsion could be assessed non-invasively in humans. In healthy volunteers, the relation was close to what was predicted by a mathematical model of LV mechanics, and also close to what was found earlier in experiments on animals. © 1997 Elsevier Science Ltd.

Keywords: Left ventricle; Torsion; Cardiac function; Systole; MR tagging.

INTRODUCTION

During contraction of the left ventricle (LV), circumferential strain in the subendocardial layers is about twice as much as in the subepicardial layers (Clark *et al.*, 1991). The arrangement of myocardial fibers, however, is such that during ejection the transmural distribution of strain along the fiber direction is practically uniform (Arts and Reneman, 1989). The equalization of strain is a direct consequence of torsion of the wall around the long axis, and works as follows. In the subendocardial and subepicardial layers the fibers follow helical pathways with mutually opposite pitch direction. During ejection, torsion uncoils the subepicardial helices and coils the subendocardial ones. As a consequence of torsion, subepicardial fibers experience extra shortening at the cost of lengthening of the subendocardial fibers. Thus, torsion is a means to redistribute strain over the wall. Without torsion the subendocardial fibers would shorten much more than the subepicardial ones. In a mathematical model of LV wall mechanics (Arts *et al.*, 1984; Arts and Reneman, 1989) it has been found that appropriate tuning of torsion to the ejected volume can cancel these transmural differences. In animal experiments the predicted relation between torsion and ejected volume is confirmed to exist (Arts *et al.*, 1984).

Cardiac disorders such as myocardial ischemia or infarction, and hypertrophic cardiomyopathy have been shown to alter the pattern of myocardial deformation (Lima *et al.*, 1995; Maier *et al.*, 1992; Prinzen *et al.*, 1989; Young *et al.*, 1994). Such disorders cause non-uniformities in fiber shortening, which is likely to result in disruption of the fine tuning of torsion to changes in ejected volume. We propose to use our foreknowledge about regular cardiac motion to enhance sensitivity in detecting motion disorders. As a first step the normal pattern of contraction has to be assessed with tools available to the clinic.

Developments in Magnetic Resonance Imaging (MRI) have provided powerful tools to quantify LV deformation (Buchalter *et al.*, 1990; Maier *et al.*, 1992; Young *et al.*, 1994; Zerhouni *et al.*, 1988). With the Magnetic Resonance Tagging technique a grid of tags is attached non-invasively to the heart by means of Spatial Modulation of the Magnetization (SPAMM). The grid deforms with the tissue and can be visualized for a period of about 300 ms (Fig. 1). This period is generally long enough to cover the ejection phase.

The aim of this study was to determine the magnitude and range of the normal pattern of cardiac deformation, as expressed in terms of torsion and changes in cross-sectional area of the LV. In healthy volunteers cardiac motion was measured with MR tagging. A kinematic model was used to extract the change in cavity area and torsion from the motion data. To judge our understanding of cardiac motion, the deformation as measured was compared with the deformation as predicted by a mathematical model of LV wall mechanics.

Received in final form 20 *September* 1996.
Author to whom correspondence should be addressed: Theo Arts, Department of Biophysics, Maastricht University, P.O. Box 616, 6200 MD Maastricht, The Netherlands.

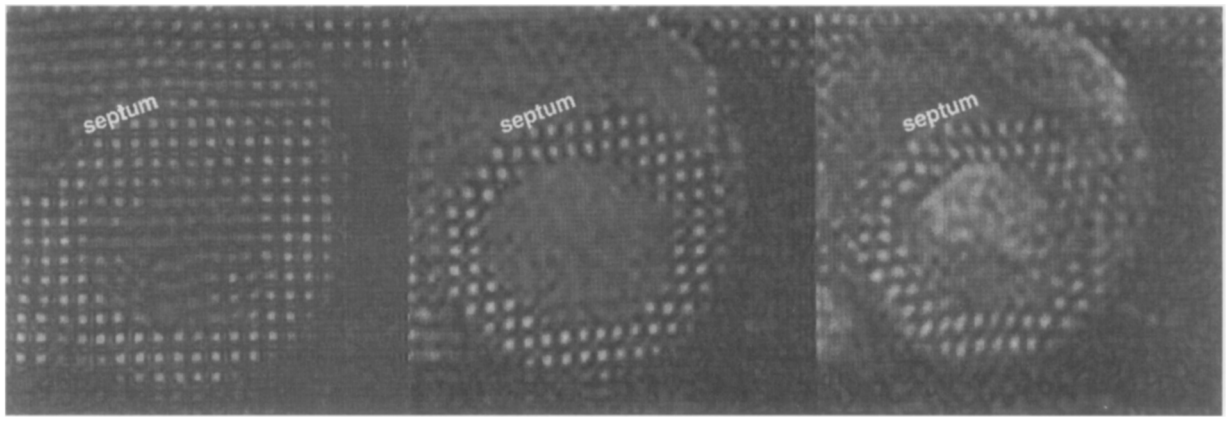

Fig. 1. MR-tagged short-axis images of the contracting cardiac left ventricle. Small regions of altered magnetization are visible as tags. The images were acquired at 20, 96, and 172 ms after the R-wave in the ECG. The motion of the tags corresponds to myocardial deformation. Gradually the tags fade away. In the left ventricular cavity they disappear shortly after excitation of the grid due to the ejection of blood.

MR MEASUREMENTS

MR-tagged images were obtained in nine healthy volunteers at two parallel short-axis cross-sections, located at about 2 and 4 cm below the base of the LV, using a 0.5 T (Tesla) MR imaging system (Philips Gyroscan T5-II, Philips Medical Systems, Best, The Netherlands). The locations of these cross-sections were determined using a compound angulation method in which transverse and coronal-angulated images were acquired sequentially. Slice thickness was 8 mm. From both cross-sections two sequential image series were acquired in order to cover the entire ejection phase. The applied intertag distance was 5 mm and the time interval between two consecutive images was about 20 ms. In addition, non-tagged MR images were obtained at the same short-axis cross-sections.

Tags, defined as the bright spots in between the dark lines, were enhanced by matched spatial bandpass filtering of the separate images. In the two-dimensional spatial frequency domain the information of the deformed grid of tags was restricted to regions around the lowest harmonics, i.e. eight regions arranged symmetrically around the origin. Only these regions were passed by the filter. The lowest spatial frequencies located around the origin, responsible for the large bright area in the LV cavity, were also filtered out. After filtering the images were thresholded. The position of a tag was calculated as the center of gravity of the pixels of the thresholded tag. Corresponding tags in consecutive images were identified by the Iterative Lower Rank Approximation procedure developed by Muijtjens *et al.* (1993). By this procedure, coordinates of missing tags in the tracks were estimated assuming coherence of motion in the set of tags.

The tag tracks thus found (Fig. 2) were fitted to a kinematic model of LV cross-sectional motion using a least squares method. In the kinematic model it was assumed that normal LV deformation is rotationally symmetric, wall volume is constant, and during contraction shortening of base to apex segment length is 65% of outer circumference shortening (Feigl and Fry, 1964). Then, the

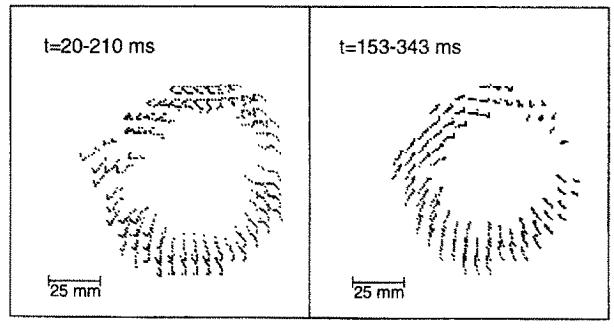

Fig. 2. Tags in MR-tagged short-axis images of the ejecting human left ventricle were followed in time. The position of a tag is represented by its center of gravity in a thresholded image. Left panel: tag positions in a series of images covering the early phase of ejection (20–210 ms after the R-wave in the ECG). Three of the images in this series were shown in Fig. 1. Right panel: tag positions in a series of images covering the late phase of ejection (153–343 ms after the R-wave in the ECG). The tagging grid is rectangular in the first image of both series. Then the grid deforms along with the tissue. The general motion of the tags is inward, so time can be followed in the figures by following the tracks inward.

radial motion of all points in a cross-section of the wall can be described completely by the motion of the outer radius. At a conveniently chosen reference time the inner and outer radii of the LV were measured directly in the non-tagged images of both cross-sections. The reference time was chosen at about mid-ejection, so that parameter values were estimated with respect to the tag positions in the middle of the trajectory of deformation.

For a mathematical description of the deformation we represent LV cross-sectional displacement by $\Delta\mathbf{M}_t$, rotation angle by Φ_t, and the outer radius by $R_{o,t}$. A point in the LV wall with position vector $\mathbf{x}_{ref}$ at the reference time (ref) moves to the position $\hat{\mathbf{x}}_t$ at time t according to the kinematic model (Appendix A):

$$\hat{\mathbf{x}}_t = \mathbf{M}_{ref} + \Delta\mathbf{M}_t + \sqrt{R_{o,t}^2 - (R_{o,ref}^2 - r_{ref}^2)\left(\frac{R_{o,ref}}{R_{o,t}}\right)^{0.65}} \times \begin{bmatrix} \cos(\phi_{ref} + \Phi_t) \\ \sin(\phi_{ref} + \Phi_t) \end{bmatrix}. \quad (1)$$

The symbols (r_{ref}, ϕ_{ref}) refer to the polar coordinates of $\mathbf{x}_{ref}$ with respect to the center ($\mathbf{M}_{ref}$) of the LV cross-section at the reference time. Thus calculated positions of all tags were compared with the measured positions ($\mathbf{x}_t$) of the tags at time t and a least squares fit was used to estimate the kinematic parameters $\mathbf{M}_{ref}$, $\Delta\mathbf{M}_t$, Φ_t and $R_{o,t}$. Note that the two sequential image series were treated separately, each with its own reference tag positions. The reference time was the same for both image series.

After the kinematic parameters were estimated for both cross-sections, torsion and area ejection of the LV were quantified. Torsion was calculated as the axial gradient in rotation angle multiplied by the average of the outer radii in both sections:

$$\text{Torsion}_t = \frac{\Phi_t^l - \Phi_t^u}{Z} \cdot (R_{o,t}^l + R_{o,t}^u)/2, \qquad (2)$$

with u and l denoting the upper and lower LV cross-section, respectively, and Z is the distance between the cross-sections. Physically, this measure of torsion may be interpreted as the shear angle on the epicardial surface between both cross-sections. LV area ejection was quantified as the natural logarithm of the ratio of cavity area (A_c) to wall area (A_w) and was calculated using the average inner ($R_{i,t}$) and outer ($R_{o,t}$) radii in the two cross-sections:

$$\ln\left[\frac{A_c}{A_w}\right]_t = \ln\left[\frac{(R_{i,t}^l + R_{i,t}^u)^2}{(R_{o,t}^l + R_{o,t}^u)^2 - (R_{i,t}^l + R_{i,t}^u)^2}\right]. \qquad (3)$$

The inner radius was determined as a function of the estimated outer radius by (Appendix A):

$$R_{i,t} = \sqrt{R_{o,t}^2 - (R_{o,ref}^2 - R_{i,ref}^2)\left(\frac{R_{o,ref}}{R_{o,t}}\right)^{0.65}}. \qquad (4)$$

Note that the inner and outer radii are measured once at the reference time. For the other moments in time these radii are calculated from the changes in position of the tags, assuming that the radii follow the motion of the grid of tags.

MATHEMATICAL MODEL OF LEFT VENTRICULAR MECHANICS

Previously, torsion and area ejection of the contracting LV were also calculated using a mathematical model of LV wall mechanics (Arts and Reneman, 1989). In this model the LV was represented by a thick-walled anisotropic cylinder, including the mitral valve—papillary muscle system. Fiber orientation in the wall was chosen such that the transmural distribution of fiber stress was as uniform as possible. The resulting transmural course of muscle fiber orientation was not significantly different from anatomical findings. The used relation between stress and strain in the myocardial tissue was physiological. Furthermore, the LV was loaded with a physiological hemodynamic impedance. LV geometry and hemodynamic variables were calculated throughout the cardiac cycle using equilibria of forces and torques.

RESULTS

MR-tagged images were obtained in nine healthy volunteers at two parallel short-axis cross-sections located in the equatorial region of the LV. For each cross-section the displacement, rotation and area ejection parameters were estimated. Figure 3 shows examples of time courses of rotation angles and inner and outer radii. Rotation angles from the beginning to the end of ejection were -0.056 ± 0.049 rad (mean $\pm$ S.D.) for the upper cross-section, and 0.035 ± 0.054 rad in the opposite direction for the lower cross-section, as viewed from apex to base, counterclockwise positive. The outer radius decreased from 36.0 ± 2.7 mm to 32.3 ± 2.7 mm for the upper cross-section, and from 35.4 ± 3.0 mm to 31.4 ± 2.5 mm for the lower cross-section. The inner radii decreased relatively more: from 25.2 ± 1.5 mm to 18.1 ± 2.2 mm for the upper cross-section, and from 23.9 ± 2.1 mm to 15.5 ± 2.0 mm for the lower one. Torsion and area ejection were calculated as a function of time (Fig. 4). Note the similarity in the time courses of torsion and the logarithm of normalized cavity area during the ejection phase, except for the sign. During ejection, torsion increased by an amount of 0.146 ± 0.028 rad. The ratio of cavity area to wall area decreased from 0.92 ± 0.16 to 0.41 ± 0.12.

Figure 5 shows changes of torsion as a function of the logarithm of normalized cavity area for the nine volunteers. For the purpose of proper presentation the curves are shifted arbitrarily along the torsion axis. During the ejection phase the relation between torsion and the logarithm of normalized cross-sectional cavity area was practically linear. Regression analysis, applied to the parts of the curves associated with the ejection phase, rendered a slope of -0.173 ± 0.024 rad.

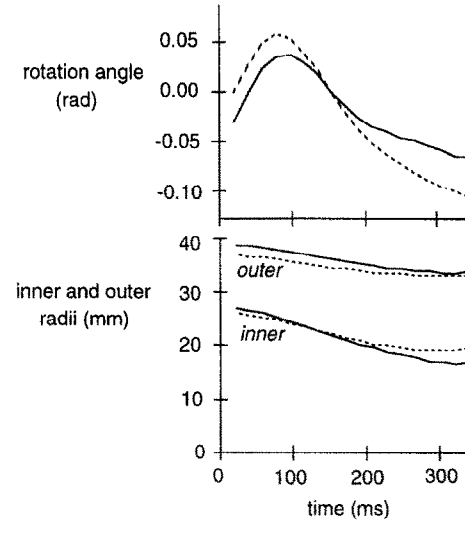

Fig. 3. Rotation angles and inner and outer radii of two left ventricular short-axis cross-sections as a function of time for a healthy volunteer. Time 0 refers to the R-wave in the ECG. Dashed lines: upper cross-section. Solid lines: lower cross-section. Rotation angles are set to zero at the reference time at about mid-ejection. Differences in rotation angles between the cross-sections are associated with torsion of the left ventricle.

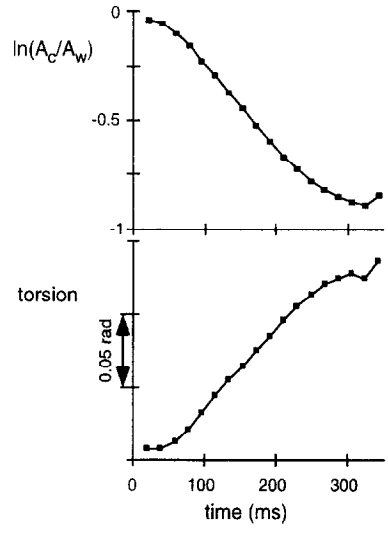

Fig. 4. Time courses of area ejection (upper panel) and torsion (lower panel) of the left ventricle as measured by means of MRI. Time 0 refers to the R-wave in the ECG. Area ejection was expressed as the logarithm of the ratio of cavity area (A_C) to wall area (A_W). Torsion was represented by the shear angle on the epicardium. Only changes in the torsion angle are considered relevant.

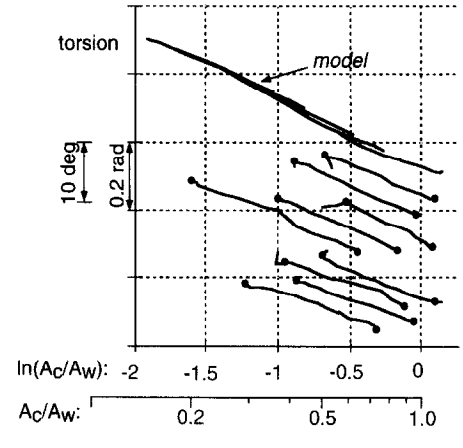

Fig. 5. Relationship between torsion and area ejection during systole as measured by means of MRI, and according to a mathematical model of left ventricular mechanics. Area ejection was expressed as the logarithm of the ratio of cavity area (A_C) to wall area (A_W). Torsion was represented by the shear angle on the epicardium. The curves obtained from the volunteers are marked by dots, indicating the beginning and end of the ejection phase. The other curves are a result of simulations.

Also in Fig. 5, five simulations of torsion are shown as a function of area ejection, each curve having a different end-diastolic cavity volume. The ratio of cavity area to wall area at the beginning of the ejection phase ranged from 0.36 to 1.15, and at the end of ejection from 0.15 to 0.57. The mathematically predicted curves were similar to the measured curves. Linear regression, applied to the simulations, rendered a slope of -0.194 ± 0.026 rad.

DISCUSSION

In healthy volunteers we found a systematic relationship between torsion and the ratio of cavity to wall cross-sectional area (A_c/A_w). Applying linear regression to torsion as a function of $\ln(A_c/A_w)$ a slope was found of -0.173 ± 0.024 rad (mean $\pm$ S.D.). In a mathematical model of LV wall mechanics this slope was predicted to be -0.194 ± 0.026 rad. The slopes in the measurements and the simulations are so close that the basic assumptions made in the model are considered to be realistic approximations.

Cardiac disorders such as myocardial ischemia or infarction, and hypertrophic cardiomyopathy are known to influence the pattern of myocardial deformation (Lima *et al.*, 1995; Maier *et al.*, 1992; Prinzen *et al.*, 1989; Young *et al.*, 1994). Therefore, a method detecting these patterns has a potential clinical use. For example, in subendocardial ischemia the subendocardial fibers will, due to loss of function, shorten less than the subepicardial fibers. This results in an increase in torsion (Prinzen *et al.*, 1984), which can be understood as follows. In the healthy heart the fibers in the inner and outer layers of the wall exert opposite torques. Torques due to the outer layers are larger than torques due to the inner layers because of the longer lever. This causes torsion to occur in favor of the outer layers. During subendocardial ischemia the counteracting torque of the inner layers is diminished and therefore torsion will increase. Added to the reduced fiber shortening during ischemia, the absolute value of the slope of the relation between torsion and area ejection is expected to increase. Furthermore, a kinematic model appears to be a useful tool in describing myocardial deformation. Once the normal deformation of the healthy heart has been accurately described, residuals from this normal pattern give information about pathology. Furthermore, these residuals can be described in the kinematic model by adding more parameters. In this way foreknowledge about regular cardiac motion can be used to enhance sensitivity in detecting motion disorders.

Assessment of the relation between dimensionless representations of torsion and contraction has received little attention in literature. In several reports torsion and contraction were investigated separately (Buchalter *et al.*, 1994; Gibbons Kroeker *et al.*, 1993; Hansen *et al.*, 1991; Ingels *et al.*, 1989; Ohayon and Chadwick, 1988; Rademakers *et al.*, 1992; Young *et al.*, 1994). Arts *et al.* (1984) measured the relation between torsion and contraction echographically in dogs. Furthermore, they compared their results with the predictions of a mathematical model of LV mechanics. Contraction was described by shortening of the inner circumference of the LV. The mathematical model predicted an approximately linear relationship between torsion and inner circumference shortening, with a slope of 2.37 ± 0.36 rad^{-1}. Echographically a slope of 2.31 ± 0.23 rad^{-1} (mean $\pm$ S.D.) was determined in a series of 11 measurements, each based on frame-to-frame analysis of 15 cardiac cycles. On the basis of the data in the present MR experiments we calculated a slope of 2.63 ± 0.37 rad^{-1} for the nine volunteers.

The ejection fraction (EF) is a clinical parameter which is widely used to characterize cardiac function. Although determination of the ejection fraction was not our primary goal, an estimate can be given using the cross-sectional area changes we determined (Appendix B):

$$EF = 100\% \left(1 - \frac{A_{c,ee}/A_{w,ee}}{A_{c,be}/A_{w,be}}\right), \quad (5)$$

with be and ee denoting the beginning and end of the ejection phase. The average ejection fraction thus obtained was 56.4 ± 6.1% for the nine volunteers, which is similar to values reported in literature (Semelka *et al.*, 1990).

The accuracy of visual estimation of inner and outer radii of an LV cross-section is of the order of ±1 mm. Changes in the radii between two consecutive images are often less than 1 mm. We estimated the radii visually at only one reference time. Using these estimates, changes in the radii were determined based on tag motion with the help of a kinematic model. Inner and outer radii thus found at the other times were within the range of accuracy of visual estimation at those times. Errors of ±1 mm in the visually estimated radii at the reference time introduced errors of approximately 10% in the slope of the linearized relation between torsion and area ejection.

We acquired images only from short-axis cross-sections of the LV, so no information was obtained about motion in the long-axis direction. The assumption was made in the kinematic model that shortening of base to apex segment length is 65% of outer circumference shortening. This value is based on animal experiments (Feigl and Fry, 1964). For comparison, if no axial shortening is assumed in the kinematic model, the slope of the relation between torsion and area ejection decreases by about 12%. Since in the healthy heart axial shortening does occur, the systematic error in the slope due to our assumption is not expected to be larger than about 5%.

Short-axis images of the LV were acquired from two fixed planes. Due to rigid body motion and shortening of the LV in the long-axis direction the cross-sections of the LV that were visualized changed in time. The myocardial tissue was tagged by selectively saturating planes orthogonal to the image plane. This was done in two perpendicular directions resulting in more or less cylindrical regions of unsaturated tissue orthogonal to the image plane, here called tag lines. The intersection of such a tag line with the image plane determines the location of a tag in the image. Because of rigid body motion and deformation of the LV the intersection of a tag line with the image plane changes in time. In this respect we made the assumption that in the equatorial region area ejection as well as torsion were independent of long-axis position (Buchalter *et al.*, 1990). As a result, in the analysis rigid body displacement of the LV does not influence the calculation of area ejection and torsion. Measurement of torsion is also not influenced by axial shortening, as shown below. Physically, torsion is represented by the tangent of the shear angle at the epicardial surface. At end-diastole the tags are alligned with the long-axis, perpendicular to both short-axis cross-sectional planes. The intersections of the tags with the short-axis planes are detected, and their position is measured. The distance between these planes is fixed. So, the tangent of the shear angle is measured directly, meaning that the used measure of torsion is not influenced by the occurrence of axial shortening.

It is concluded that in systole the relation between torsion and area ejection is common to all left ventricles in healthy humans. This relation appeared close to predictions made by a mathematical model of LV wall mechanics. Since equilibria of forces in the wall were essential to this model, in the real heart the same equilibria are likely to play an important role.

REFERENCES

Arts, T., Meerbaum, S., Reneman, R. S. and Corday, E. (1984) Torsion of the left ventricle during the ejection phase in the intact dog. *Cardiovasc. Res.* **18,** 183–193.

Arts, T. and Reneman, R. S. (1989) Dynamics of left ventricular wall and mitral valve mechanics—a model study. *J. Biomechanics* **22,** 261–271.

Buchalter, M. B., Rademakers, F. E., Weiss, J. L., Rogers, W. J., Weisfeldt, M. L. and Shapiro, E. P. (1994) Rotational deformation of the canine left ventricle measured by magnetic resonance tagging: effects of catecholamines, ischaemia, and pacing. *Cardiovasc. Res.* **28,** 629–635.

Buchalter, M. B., Weiss, J. L., Rogers, W. J., Zerhouni, E. A., Weisfeldt, M. L., Beyar, R. and Shapiro, E. P. (1990) Noninvasive quantification of left ventricular rotational deformation in normal humans using magnetic resonance imaging myocardial tagging. *Circulation* **81,** 1236–1244.

Clark, N. R., Reichek, N., Bergey, P., Hoffman, E. A., Brownson, D., Palmon, L. and Axel, L. (1991) Circumferential myocardial shortening in the normal human left ventricle—Assessment by magnetic resonance imaging using spatial modulation of magnetization. *Circulation* **84,** 67–74.

Feigl, E. O. and Fry, D. L. (1964) Intramural myocardial shear during the cardiac cycle. *Circ. Res.* **14,** 536–540.

Gibbons Kroeker, C. A., Ter Keurs, H. E. D. J., Knudtson, M. L., Tyberg, J. V. and Beyar, R. (1993) An optical device to measure the dynamics of apex rotation of the left ventricle. *Am. J. Physiol.* **265,** H1444–H1449.

Hansen, D. E., Daughters, G. T., Alderman, E. L., Ingels, N. B., Stinson, E. B. and Miller, D. C. (1991) Effect of volume loading, pressure loading, and isotropic stimulation on left ventricular torsion in humans. *Circulation* **83,** 1315–1326.

Ingels, N. B., Hansen, D. E., Daughters, G. T., Stinson, E. B., Alderman, E. L. and Miller, D. C. (1989) Relation between longitudinal, circumferential, and oblique shortening and torsional deformation in the left ventricle of the transplanted human heart. *Circ. Res.* **64,** 915–927.

Lima, J. A. C., Ferrari, V. A., Reichek, N., Kramer, C. M., Palmon, L., Llaneras, M. R., Tallant, B., Young, A. A. and Axel, L. (1995) Segmental motion and deformation of transmurally infarcted myocardium in acute postinfarct period. *Am. J. Physiol.* **268,** H1304–H1312.

Maier, S. E., Fischer, S. E., McKinnon, G. C., Hess, O. M., Krayenbuehl, H. P. and Boesiger, P. (1992) Evaluation of left ventricular segmental wall motion in hypertrophic cardiomyopathy with myocardial tagging. *Circulation* **86,** 1919–1928.

Muijtjens, A. M. M., Roos, J. M. A., Arts, T., Hasman, A. and Reneman, R. S. (1993) Extrapolation of incomplete marker tracks by lower rank approximation. *Int. J. Biomed. Comput.* **33,** 219–239.

Ohayon, J. and Chadwick, R. S. (1988) Theoretical analysis of the effects of a radial activation wave and twisting motion on the mechanics of the left ventricle. *Biorheology* **25,** 435–447.

Prinzen, F. W., Arts, T., Hoeks, A. P. G. and Reneman, R. S. (1989) Discrepancies between myocardial blood flow and fiber shortening in the ischemic border zone as assessed with video mapping of epicardial deformation. *Eur. J. Physiol.* **415,** 220–229.

Prinzen, F. W., Arts, T., Van der Vusse, G. J. and Reneman, R. S. (1984) Fiber shortening in the inner layers of the left ventricular wall as assessed from epicardial deformation during normoxia and ischemia. *J. Biomech.* **17,** 801–811.

Rademakers, F. E., Buchalter, M. B., Rogers, W. J., Zerhouni, E. A., Weisfeldt, M. L., Weiss, J. L. and Shapiro, E. P. (1992) Dissociation between left ventricular untwisting and filling—accentuation by catecholamines. *Circulation* **85,** 1572–1581.

Semelka, R. C., Tomei, E., Wagner, S., Mayo, J., Kondo, C., Suzuki, J.-I., Caputo, G. R. and Higgins, C. B. (1990) Normal left ventricular dimensions and function: interstudy reproducibility of measurements with cine MR imaging. *Radiology* **174,** 763–768.

Young, A. A., Imai, H., Chang, C. N. and Axel, L. (1994) Two-dimensional left ventricular deformation during systole using magnetic resonance imaging with spatial modulation of magnetization. *Circulation* **89,** 740–752.

Young, A. A., Kramer, C. M., Ferrari, V. A., Axel, L. and Reichek, N. (1994) Three-dimensional left ventricular deformation in hypertrophic cardiomyopathy. *Circulation* **90,** 854–867.

Zerhouni, E. A., Parish, D. M., Rogers, W. J., Yang, A. and Shapiro, E. A. (1988) Human heart: tagging with MR imaging—a method for noninvasive assessment of myocardial motion. *Radiology* **169,** 59–63.

APPENDIX A

During ventricular contraction wall volume is approximately constant. Thus:

$$(R_{o,t}^2 - r_t^2)H_t = (R_{o,ref}^2 - r_{ref}^2)H_{ref} \tag{A1}$$

with R_o the outer radius of the LV cross-section, r the distance of a point in the myocardial wall to the center of the LV cross-section, H the length of a base to apex segment, and t and ref denoting time t and a reference time, respectively. Assuming shortening of base to apex segment length to be 65% of outer circumference shortening, it follows that

$$r_t = \sqrt{R_{o,t}^2 - (R_{o,ref}^2 - r_{ref}^2)\left(\frac{R_{o,ref}}{R_t}\right)^{0.65}}. \tag{A2}$$

Besides circumferential shortening, the LV cross-section undergoes rigid body rotation (Φ) and displacement ($\Delta\mathbf{M}$) with respect to the center of the cross-section at the reference time ($\mathbf{M}_{ref}$). Successive application of the preceding circumferential shortening, rotation, and displacement to a point in the myocardial wall gives equation (1). Equation (4) is obtained by substituting the inner radius of the LV cross-section (R_i) for r_t in equation (A2).

APPENDIX B

Because we only acquired images from short-axis cross-sections we cannot determine the ejected volume fraction (EF) directly. An estimate of EF can be obtained by assuming that the shape of the left ventricle is ellipsoidal, and that the cross-sectional area changes are measured at the equator. Then it holds that

$$\frac{V_{c,ee}}{V_{c,be}} = \frac{\frac{4}{3}\pi R_{i,ee}{}^2 H_{ee}}{\frac{4}{3}\pi R_{i,be}{}^2 H_{be}} = \frac{A_{c,ee}H_{ee}}{A_{c,be}H_{be}} = \frac{A_{c,ee}H_{ee}}{A_{c,be}H_{be}}\frac{A_{w,be}H_{be}}{A_{w,ee}H_{ee}} = \frac{A_{c,ee}/A_{w,ee}}{A_{c,be}/A_{w,be}}, \tag{B1}$$

with V_c representing the left ventricular cavity volume, R_i the short-axis length of the cavity, and H the long-axis length. The symbols A_c and A_w refer to the cross-sectional cavity and wall areas, respectively, and be and ee denote the beginning and end of the ejection phase. Wall volume was assumed to be constant during ejection so that $A_w H$ remains constant. Then for the ejection fraction (EF), equation (5) follows. Note that long-axis shortening is implicitly accounted for in this approach, which is reflected in the different values for cross-sectional wall area for the beginning and end of ejection.